

**Giant quantized Goos-Hänchen effect on the surface of graphene in the quantum Hall regime**

Weijie Wu, Shizhen Chen, Chengquan Mi, Wenshuai Zhang, Hailu Luo,\* and Shuangchun Wen  
*Laboratory for Spin Photonics, School of Physics and Electronics, Hunan University, Changsha 410082, China*

(Received 1 August 2017; published 6 October 2017)

We theoretically predict a giant quantized Goos-Hänchen (GH) effect on the surface of graphene in the quantum Hall regime. The giant quantized GH effect manifests itself as an angular shift whose quantized step reaches the order of mrad for light beams impinging on a graphene-on-substrate system. The quantized GH effect can be attributed to quantized Hall conductivity, which corresponds to the discrete Landau levels in the quantum Hall regime. We find that the quantized step can be greatly enhanced for incident angles near the Brewster angle. Moreover, the Brewster angle is sensitive to the Hall conductivity, and therefore the quantized GH effect can be modulated by the Fermi energy and the external magnetic field. The giant quantized GH effect offers a convenient way to determine the quantized Hall conductivity and the discrete Landau levels by a direct optical measurement.

DOI: [10.1103/PhysRevA.96.043814](https://doi.org/10.1103/PhysRevA.96.043814)

**I. INTRODUCTION**

The well-known Snell's law and Fresnel formulas provide a clear geometrical-optics picture to describe the interaction of a plane wave with an interface [1,2]. In 1947, the spatial shift of a beam of light in total internal reflection from a dielectric surface was demonstrated, which does not follow perfectly the geometrical-optics prediction. This spatial shift was first observed by Goos and Hänchen [3], and was therefore referred to as the Goos-Hänchen (GH) effect. In a simple explanation, such a spatial GH shift is attributed to the penetration of an evanescent field. For the past few decades, the spatial GH shift has been studied in a variety of systems, such as plasmonics [4–6], metamaterials [7–18], and quantum systems [19,20]. In addition, an angular GH shift has been predicted for the case of partial reflection, which can be explained as the Fresnel filtering [21,22]. This remarkable deviation from geometrical optics has been measured experimentally on the surface of bulk crystals [23–26].

Recently, graphene, as a two-dimensional atomic crystal, has received considerable attention due to its extraordinary electronic and photonic properties [27–29]. It has been demonstrated that the Fresnel formulas based on certain thicknesses and effective refractive indices fail to perfectly explain the light-matter interaction of graphene. However, the Fresnel formulas based on a zero-thickness interface can give a complete and convincing description of all the experimental observations [30,31]. It would be interesting to see how the GH effect occurs on a zero-thickness interface of graphene. More recently, the quantized spatial shifts in the GH effect have been theoretically predicted in the quantum Hall regime of graphene-substrate systems [32]. However, the quantized steps are just a fraction of a micrometer in the terahertz regime. Therefore, the enhancement of this tiny effect is still a challenging problem.

In this paper, we theoretically predict a giant quantized GH effect on the surface of graphene in the quantum Hall regime. A general propagation model is established to describe the GH shifts on a surface graphene-on-substrate system and freestanding graphene. Based on this model, both the spatial

and the angular GH shifts are obtained when a light beam impinges on the surface of graphene. Most previous works have demonstrated that the beam shifts can be significantly enhanced near the Brewster angles on the surfaces of bulk crystals [33–43]. As expected, giant angular GH shifts are also obtained on the surface graphene. More importantly, we find that the quantized steps in angular GH shifts can be significantly enhanced and reach the order of mrad. Furthermore, we examine the role of Hall conductivity in the quantized GH effect. We believe this work to be of fundamental significance and may provide a possible scheme for the direct optical measurement of the quantized effect in graphene.

**II. GENERAL PROPAGATION MODEL**

We begin by analyzing optical reflection from a planar interface of a graphene-substrate system. Here, the semiclassical model is applied to describe the quantized GH effect on the surface of graphene in the quantum Hall regime. In the semiclassical model, the electromagnetic field is treated classically and the graphene system is described quantum mechanically. In the quantum Hall regime, both longitudinal conductivity and transverse Hall conductivity can be obtained from the Kubo formula with a quantum description [44,45]. The light-matter interaction on the surface of graphene can be described with Fresnel's equations obtained by solving Maxwell's equations and boundary conditions. The semiclassical model has been applied to explain the quantized Faraday and Kerr effects in graphene. Theoretical results that coincide well with the experimental results have been demonstrated [46–48]. In our case, we apply the same model to explain the quantized GH effect in the quantum Hall regime.

Figure 1 illustrates a monochromatic Gaussian beam of light with a finite beam width and nontotal reflection impinging from air to a planar interface of a graphene-substrate system. The  $z$  axis of the laboratory Cartesian frame  $(x, y, z)$  is normal to the air-graphene interface ( $z = 0$ ), which separates empty space (typically air), where  $z < 0$ , from a substrate that is covered with a graphene sheet, where  $z > 0$ , and a static magnetic field  $B$  is applied along the  $z$  axis [49]. We use the coordinate frames  $(x_i, y_i, z_i)$  and  $(x_r, y_r, z_r)$  to denote the incident beam and the reflected one, respectively. The electric

\*hailuluo@hnu.edu.cn

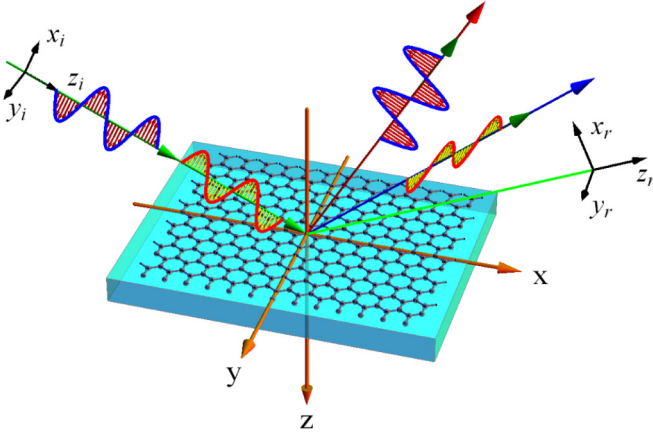


FIG. 1. Schematic representation of the wave reflection at a graphene-substrate interface. The homogeneous and isotropic substrate is covered by a graphene sheet. An external imposed static magnetic field  $B$  is applied perpendicular to the interface. On the reflecting surface, the giant angular GH shifts occur at different values, where the shift of parallel polarized reflection is greater than perpendicular polarized reflection.

field amplitude of such a beam can be written as [50–52]

$$\tilde{\mathbf{E}}_i \propto \exp\left[ikz_i - \frac{k}{2} \frac{x_i^2 + y_i^2}{Z_R + iz_i}\right] \times (\hat{\mathbf{x}}_i f_p + \hat{\mathbf{y}}_i f_s), \quad (1)$$

where  $Z_R = \pi w_0^2/\lambda$  is the Rayleigh range, and the vectors  $\hat{\mathbf{x}}, \hat{\mathbf{y}}$  represent the directions parallel and perpendicular to the incidence plane, respectively. The polarization of the beam is determined by the complex-valued unit vector  $\hat{\mathbf{f}} = (f_p \hat{\mathbf{x}}_i + f_s \hat{\mathbf{y}}_i)/(|f_p|^2 + |f_s|^2)^{1/2}$ .

The reflected angular spectrum of the electric field is associated with the boundary distribution by means of the relation [53]

$$\begin{bmatrix} \tilde{\mathbf{E}}_r^p \\ \tilde{\mathbf{E}}_r^s \end{bmatrix} = \begin{bmatrix} r_{pp} & r_{ps} \\ r_{sp} & r_{ss} \end{bmatrix} \cdot \begin{bmatrix} \tilde{\mathbf{E}}_i^p \\ \tilde{\mathbf{E}}_i^s \end{bmatrix}. \quad (2)$$

Here,  $r_{pp}$  and  $r_{ss}$  denote the Fresnel reflection coefficients for parallel and perpendicular polarizations, respectively.  $r_{ps}$  and  $r_{sp}$  denote the cross polarization.

In Eq. (2), we have introduced the boundary conditions  $k_{rx} = -k_{ix}$  and  $k_{ry} = k_{iy}$ . By making use of a Taylor series expansion based on the arbitrary angular spectrum component,  $r_A$  can be expanded as a polynomial of  $k_{ix}$ ,

$$\begin{aligned} r_A(k_{ix}) &= r_A(k_{ix} = 0) + k_{ix} \left[ \frac{\partial r_A(k_{ix})}{\partial k_{ix}} \right]_{k_{ix}=0} \\ &+ \sum_{j=2}^N \frac{k_{ix}^j}{j!} \left[ \frac{\partial^j r_A(k_{ix})}{\partial k_{ix}^j} \right]_{k_{ix}=0}, \end{aligned} \quad (3)$$

where  $A \in \{pp, ss, ps, sp\}$ . Then, the reflected field can be solved by utilizing the Fourier transformations. The complex amplitude can be conveniently expressed as

$$\begin{aligned} \mathbf{E}_r(x_r, y_r, z_r) &= \iint dk_{rx} dk_{ry} \tilde{\mathbf{E}}_r(k_{rx}, k_{ry}) \\ &\times \exp[i(k_{rx}x_r + k_{ry}y_r + k_{rz}z_r)], \end{aligned} \quad (4)$$

where  $k_{rz} = \sqrt{k_r^2 - (k_{rx}^2 + k_{ry}^2)}$  and  $\tilde{\mathbf{E}}_r(k_{rx}, k_{ry})$  is the reflected angular spectrum.

From Eqs. (1)–(4), the general expression of the reflected field is determined and can be written as

$$\begin{aligned} \mathbf{E}_r &\propto \exp\left(ikz_r - \frac{k}{2} \frac{x_r^2 + y_r^2}{Z_R + iz_r}\right) \\ &\times \left\{ \hat{\mathbf{x}}_r \left[ f_p r_{pp} \left(1 - \frac{ix_r}{Z_R + iz_r} \frac{\partial \ln r_{pp}}{\partial \theta_i}\right) \right. \right. \\ &+ f_s r_{ps} \left. \left(1 - \frac{ix_r}{Z_R + iz_r} \frac{\partial \ln r_{ps}}{\partial \theta_i}\right) \right] \\ &+ \hat{\mathbf{y}}_r \left[ f_s r_{ss} \left(1 - \frac{ix_r}{Z_R + iz_r} \frac{\partial \ln r_{ss}}{\partial \theta_i}\right) \right. \\ &+ f_p r_{sp} \left. \left(1 - \frac{ix_r}{Z_R + iz_r} \frac{\partial \ln r_{ps}}{\partial \theta_i}\right) \right] \left. \right\}, \end{aligned} \quad (5)$$

where  $f_p = a_p \in \mathbb{R}$ ,  $f_s = a_s \exp(i\eta)$ .

In addition, the Fresnel reflection coefficients of the graphene-substrate system with an external imposed magnetic field can be obtained as [54–56]

$$r_{pp} = \frac{\alpha_+^T \alpha_-^L + \beta}{\alpha_+^T \alpha_+^L + \beta}, \quad (6)$$

$$r_{ss} = -\frac{\alpha_+^T \alpha_+^L + \beta}{\alpha_+^T \alpha_+^L + \beta}, \quad (7)$$

$$r_{ps} = r_{sp} = -2\sqrt{\frac{\mu_0}{\varepsilon_0}} \frac{k_{iz} k_{tz} \sigma_H}{\alpha_+^T \alpha_+^L + \beta}. \quad (8)$$

Here,  $\alpha_{\pm}^L = (k_{iz}\varepsilon \pm k_{tz}\varepsilon_0 + k_{iz}k_{tz}\sigma_L/\omega)/\varepsilon_0$ ,  $\alpha_{\pm}^T = k_{tz} \pm k_{iz} + \omega\mu_0\sigma_T$ ,  $\beta = \mu_0 k_{iz} k_{tz} \sigma_H^2/\varepsilon_0$ ,  $k_{iz} = k_i \cos \theta_i$ , and  $k_{tz} = k_t \cos \theta_t$ ;  $\theta_i$  is the refraction angle;  $\varepsilon_0, \mu_0$  are the permittivity and permeability in vacuum, respectively;  $\varepsilon$  is the permittivity of the substrate;  $\sigma_L, \sigma_T$ , and  $\sigma_H$  denote the longitudinal, transverse, and Hall conductivity, respectively.

When the external imposed magnetic field is strong enough, the Hall conductivity of the graphene is quantized in integer multiples of the fine-structure constant, and we have [32]

$$\sigma_H = 2(2n_c + 1) \text{sgn}[B] \frac{e^2}{2\pi\hbar}. \quad (9)$$

Here,  $n_c = \text{Int}[\mu_F^2/2\hbar e|B|v_F^2]$  is the number of occupied Landau levels, and  $\mu_F$  and  $v_F$  are the Fermi energy and the Fermi velocity, respectively. Obviously, the Landau levels play an important role in Hall conductivity. Note that the linear optical response of an important two-dimensional (2D) atomic crystal model of Fresnel coefficients in graphene has been developed by fixing both the surface susceptibility and the surface conductivity [57].

### III. THE GIANT ANGULAR GOOS-HÄNCHEN SHIFTS

In this section, we begin to reveal the giant angular GH shifts in graphene and discuss the relation between the shift and incident angle. Then, we try to explore the relationship between the magnitude of the Brewster angle and the external conditions of the magnetic field and Fermi energy. We now determine the centroid of the reflected beam. At any given

plane  $z_r = \text{const}$ , the longitudinal displacement of the field centroid is given by

$$D_{\text{GH}} = \frac{\int \int x_r I(x_r, y_r, z_r) dx_r dy_r}{\int \int I(x_r, y_r, z_r) dx_r dy_r}. \quad (10)$$

The beam intensity spatial profile is closely linked to the flux of the time-averaged Poynting vector  $I(x_r, y_r, z_r) \propto \bar{\mathbf{S}} \cdot \hat{\mathbf{z}}_r$ . Then, the Poynting vector related to the electromagnetic field can be obtained by  $\bar{\mathbf{S}} \propto \text{Re}(\mathbf{E}_r \times \mathbf{H}_r^*)$ . The magnetic field can be obtained by  $\mathbf{H}_r = -ik_r^{-1} \nabla \times \mathbf{E}_r$ .

In order to simplify the calculation, horizontal polarization is only considered, i.e.,  $a_p = 1$ ,  $a_s = 0$ , and  $\eta = 0$ . From Eq. (10), we get the following expression,

$$D_{\text{GH}} = \frac{2(R_{pp}^2 \varphi_{pp} + R_{ps}^2 \varphi_{ps}) Z_R}{2k(R_{ps}^2 + R_{pp}^2) Z_R + \chi_{pp} + \chi_{ps}} - z_r \frac{2(R_{pp}^2 \rho_{pp} + R_{ps}^2 \rho_{ps})}{2k(R_{ps}^2 + R_{pp}^2) Z_R + \chi_{pp} + \chi_{ps}}. \quad (11)$$

Here,  $r_A = R_A \exp(i\phi_A)$ ,  $A \in \{pp, ss, ps\}$ ,  $\rho_A = \text{Re}(\partial \ln r_A / \partial \theta_i)$ ,  $\varphi_A = \text{Im}(\partial \ln r_A / \partial \theta_i)$ , and  $\chi_A = R_A^2(\varphi_A^2 + \rho_A^2)$ . If we consider vertical polarization (i.e.,  $a_p = 0$ ,  $a_s = 1$ , and  $\eta = 0$ ), we can replace the  $pp$  with  $ss$  in the above equation. Furthermore, when vertical polarization is considered, the induced cross polarization is  $r_{sp}$  instead of  $r_{ps}$ .

Equation (11) gives the GH shift as a function of the beam propagation distance  $z_r$ . The first term is considered to represent the spatial GH shift, that is, the displacement will not change with  $z_r$ . If we use it under the conditions of total internal reflection and isotropy, we could get a result that is consistent with the Artmann formula [58]. Namely, when we make  $r_{ps} = 0$  and  $|R_{pp}| = 1$ , we will get  $D_{\text{GH}} = (\partial \phi_A / \partial \theta_i) / k$ . Then, the second term denotes the angular GH shift. For more general cases, the derivative of the Fresnel reflection coefficients can be easily simplified, so an equation can be obtained by  $\partial \ln r_A / \partial \theta_i = (\partial R_A / \partial \theta_i) / R_A + i \partial \phi_A / \partial \theta_i$ . That is, the change in phase and amplitude reflectivity is responsible for spatial and angle shifts, respectively. In the following, we limit the discussion to the angular shift only, although our results also hold for spatial shifts. An important result is obtained by

$$\Theta_{\text{GH}} = -\frac{2(R_{pp}^2 \rho_{pp} + R_{ps}^2 \rho_{ps})}{2k(R_{ps}^2 + R_{pp}^2) Z_R + \chi_{pp} + \chi_{ps}}. \quad (12)$$

As shown in Fig. 2, the angular GH shifts are quantized functions of the Fermi energy and magnetic field. Plateaulike behavior can be observed by tuning the Fermi energy  $\mu_F$  and magnetic field  $B$ . Quantized Hall conductivity can be regarded as the physical origin of plateaulike behavior. The quantized steps reach the order of mrad near the Brewster angle and can be determined by a direct optical measurement [59]. Also, due to the fact that the Hall conductivity is quantified, a quantized angular shift can be obtained. We now consider the difference in angular deviation for incidence angles near and far away from the Brewster angle [Figs. 2(a) and 2(b)]. Remarkably, the angular shift for an incidence angle near the Brewster angle will be greater, at the same Fermi energy and magnetic field.

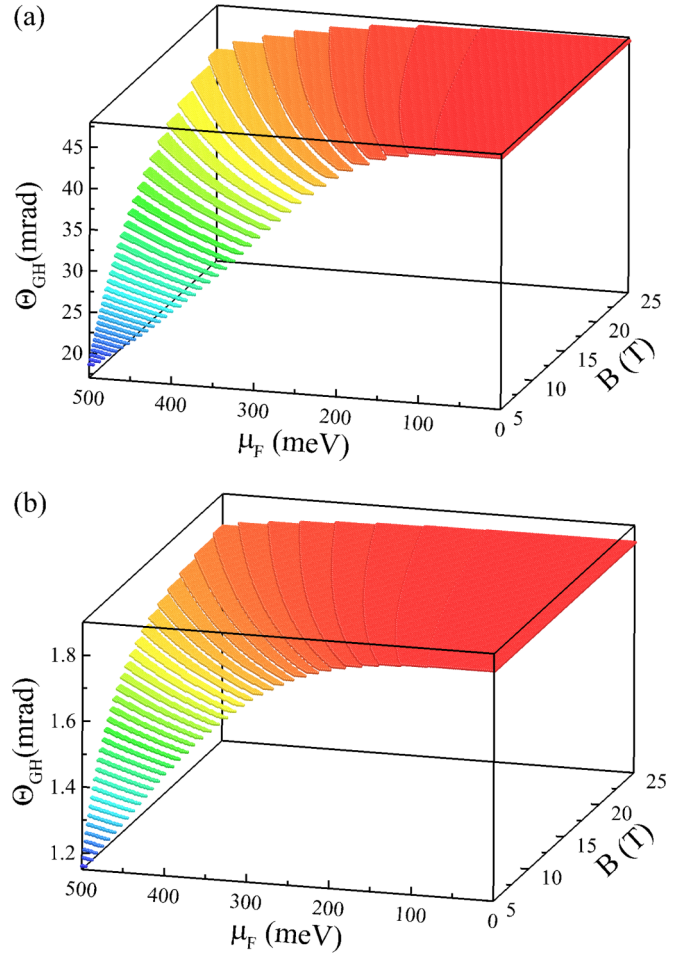


FIG. 2. Quantized angular Goos-Hänchen shifts in the graphene-substrate system as a function of Fermi energy and magnetic field. (a) The incident angles are chosen to be  $71^\circ$ , which is near the Brewster angle, and (b)  $30^\circ$ , which is far away from the Brewster angle, respectively. We assume an incident beam with  $w_0 = 1$  mm,  $\omega/2\pi = 1$  THz. The refractive index of undoped Si in the terahertz range is  $n_{\text{Si}} = 3.415$ . The temperature is chosen to be  $T = 4$  K.

If we research it further, we will find that the angular shift is not only influenced by the incident angle, but the shift is also related to the quantized Hall conductivity. In fact, the Landau levels are proportional to the Fermi energy squared, but they are inversely proportional to the magnetic field. Also, Landau levels play an important role in Hall conductivity. From Fig. 3(a), it can be seen that the Hall conductivity is decreased as the Fermi energy is decreased or the magnetic field is increased, but it is worth noting that the quantized step widths can be significantly enhanced. From Eq. (6), the quantized step widths of the Hall conductivity have a close relationship with the Brewster angle. In other words, from Fig. 3(b), the Brewster angle will dramatically change in the case of narrow quantized steps. This directly leads to the change in angular deviation. In the region of high magnetic field, this phenomenon is not obvious. This is consistent with our previous statement. Due to the widened quantized steps, the Brewster angle is insensitive to the changing magnetic field and Fermi energy. Comparing Figs. 3(c) and 3(d), it can be seen that only when we maintain

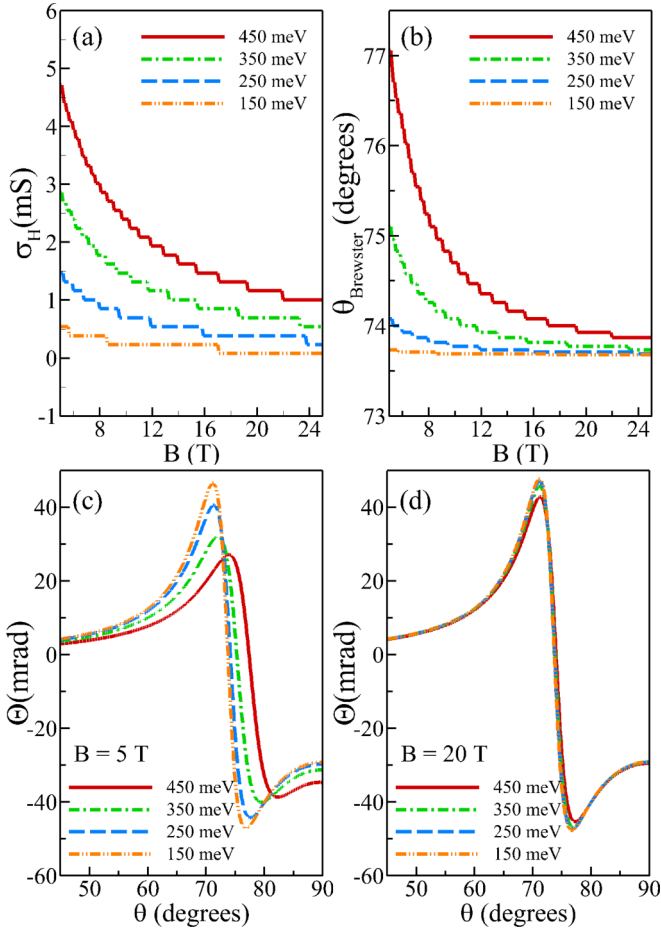


FIG. 3. The role of quantized Hall conductivity in quantized angular GH shifts. (a) Hall conductivity as a function of magnetic field in different Fermi energies,  $\mu_F = 150, 250, 350,$  and  $450$  meV. (b) The magnitudes of the Brewster angle. (c) and (d) show the changes in the angular shift at different Fermi energies and magnetic field.

the magnetic field at a relatively small value ( $B = 5$  T), which leads narrow quantized steps, will the peak of the angular shift become sensitive and move to the right with an increase in the Fermi energy. Of course, due to the magneto-optical effect, the behavior of angular deviation in a graphene-substrate system is different from that in a glass-air system [24]. In addition, the reflection coefficient  $r_{pp}$  will approach zero near the Brewster angle and change its sign across the angle, which means the electric field reverses its directions. So, when the incident angle is smaller than the Brewster angle, the angular shift is positive, and in the opposite case, the angular shift is negative. For vertical polarization, the angular deviation is very small. This rule of change seems to be a source of enlightenment for us, since if we appropriately control the external conditions, the angular shift can be modulated.

Then, we consider two special cases. First, if we used a polarizer to eliminate the cross-polarization component, namely,  $R_{ps}$ , or used a isotropic reflected medium, which also has no cross-polarization component  $R_{ps}$  and  $R_{sp}$  in the reflection matrix in Eq. (2), modified angular GH shifts can be obtained. Here, the horizontal polarization is discussed

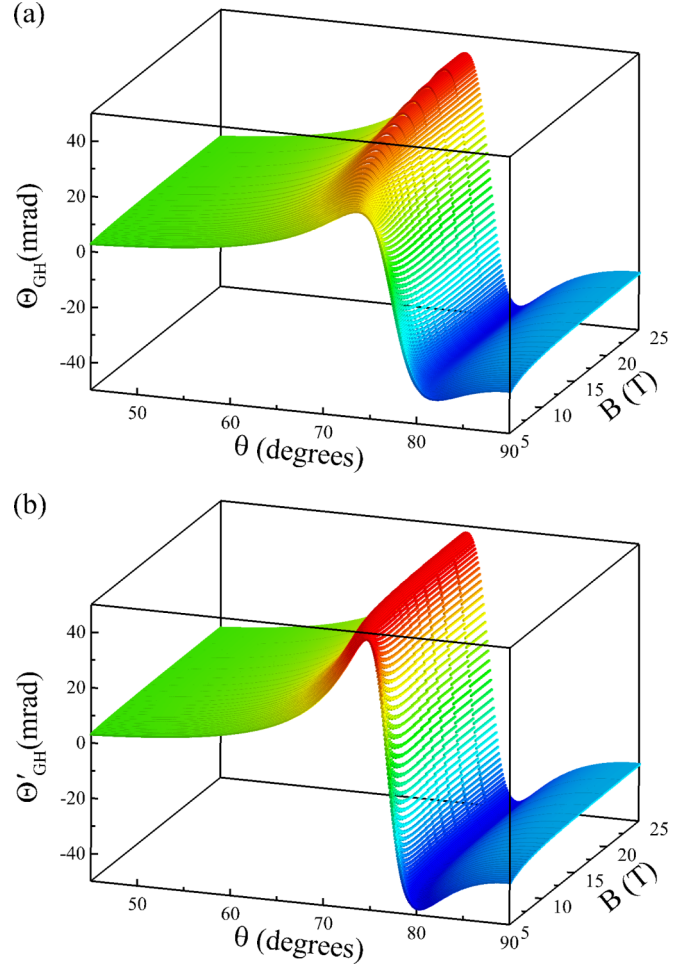


FIG. 4. Compare the original and the modified angular GH shifts. (a) The giant quantized GH shift in  $450$  meV Fermi energy (similarly hereinafter). (b) The modified angular GH shift.

only. We now consider the effect of the cross-polarization component  $R_{ps}$  on the GH shifts at different magnetic fields. So, we have a modified expression,

$$\Theta'_{GH} = -\frac{2R_{pp}^2 \rho_{pp}}{2kR_{pp}^2 Z_R + \chi_{pp}}. \quad (13)$$

Next, we compare the angular GH shift with the modified GH shift. From Fig. 4(a), there are giant quantized angular GH shifts with the change in magnetic field. The peak of  $\Theta_{GH}$  near the Brewster angle is changed with magnetic field, which is more obvious in an area with narrow quantized steps. This proves our previous statement: If quantized steps were narrowed, the angular GH shifts would be sensitive to changing magnetic field and Fermi energy. So, the position of the peak will be moved. From Fig. 4(b), the peak value of  $\Theta'_{GH}$  near the area where the magnetic field is  $5$  T is approximately  $20$  mrad larger than that of  $\Theta_{GH}$  in the corresponding range.

For a further analysis of this difference, we plot the magnitude of the cross-polarization reflection coefficients  $R_{ps}$ . As shown in Fig. 5(a), when the magnetic field is decreased, the magnitude of  $R_{ps}$  will increase. In fact, our previous statement still works. Widened quantized steps will cause  $R_{ps}$  to be



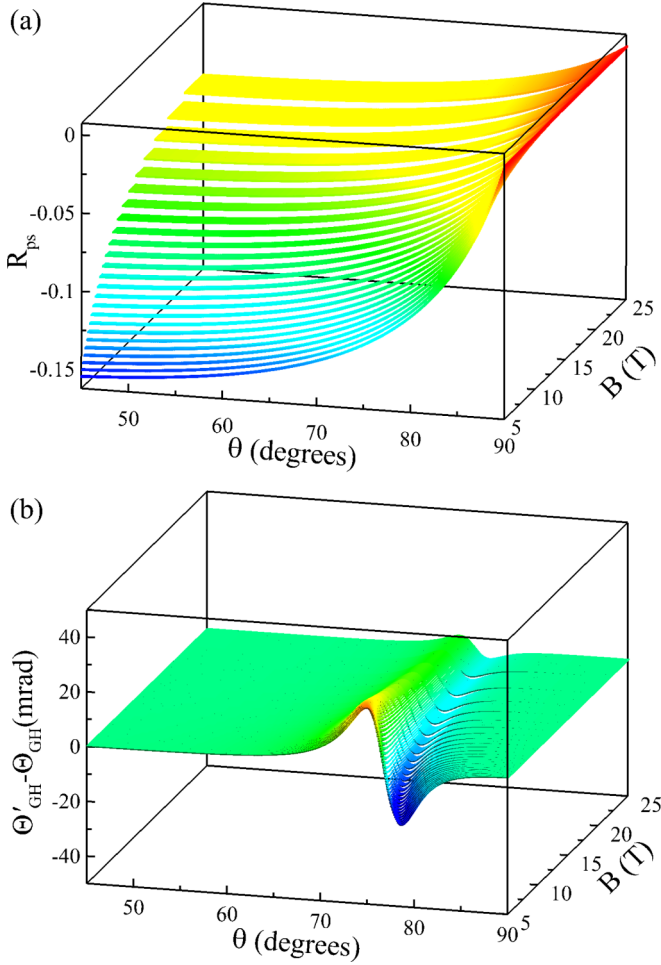


FIG. 5. The role of cross polarization in the angular GH effect. (a) Relative amplitude of the cross polarization  $R_{ps}$  as a function of angle of incidence  $\theta$  and magnetic field  $B$  for Fermi energy  $\mu_F = 450$  meV. (b) The difference between the normal GH shift  $\Theta_{GH}$  and the modified GH shift  $\Theta'_{GH}$ .

insensitive to the changing magnetic field and Fermi energy. From Fig. 5(b), it is clear that there is a significant difference between the two cases near the Brewster angle. However, it is worth noticing that the difference will decrease in the range far away from the Brewster angle or in the interval of widened quantized steps. That is to say, there are no differences (or very small differences) in the angular GH shifts in the above two ranges. At this point, we could get  $\Theta''_{GH} = -\rho_p/kZ_R$ , which is in good agreement with the theoretical result of Aiello [51]. That is,  $R_{ps}$  is responsible for the difference between the two shifts only near the Brewster angle or in the interval of narrow quantized steps.

Finally, we consider the case of freestanding graphene [60], where we can make the relative refractive index of the substrate tend to  $n = 1$ . As shown in Fig. 6, it can be seen that when the refractive index approaches 1, the magnitude of the incidence angle, which corresponds to the peak, is increased, that is, the Brewster angle will approach grazing incidence on freestanding graphene. On the other hand, when the magnetic field is high or the Fermi energy is low in the quantum Hall regime, the magnitude of the Brewster angle is decreased, and

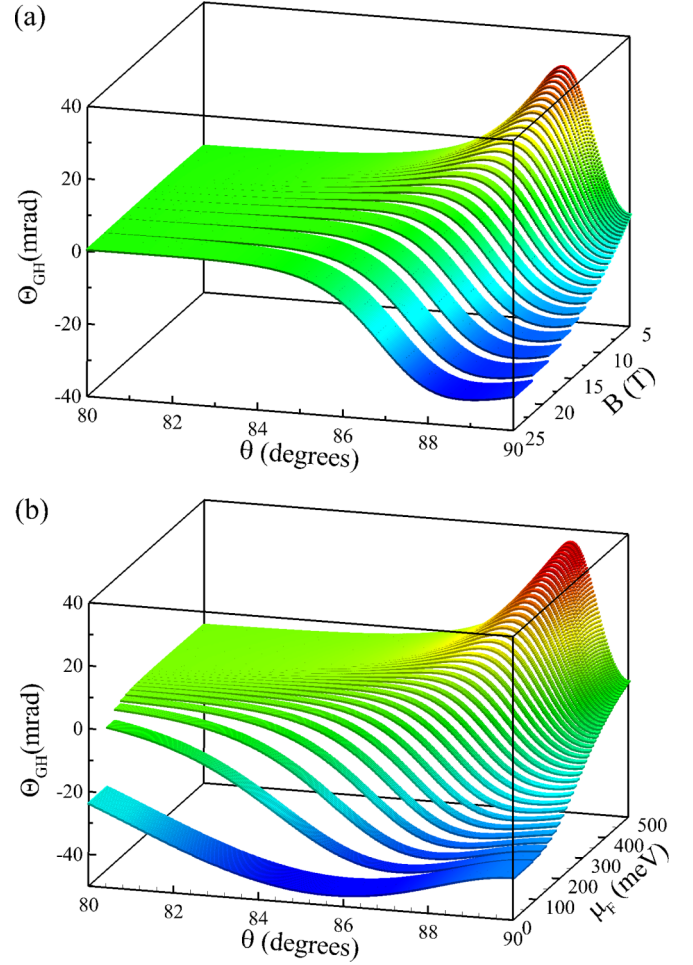


FIG. 6. Angular GH shift in freestanding graphene. (a) Angular GH shifts  $\Theta_{GH}$  as a function of incidence angle  $\theta$  and magnetic field  $B$  for Fermi energy  $\mu_F = 450$  meV. (b) Angular GH shifts  $\Theta_{GH}$  as a function of incidence angle  $\theta$  and Fermi energy  $\mu_F$  for magnetic field  $B = 5$  T. The relative refractive index of the substrate tends to  $n = 1$ ; other parameters are the same as in Fig. 2.

the quantized steps are also wide at this time, which proves that the Brewster angle in this moment is insensitive to the changing magnetic field or Fermi energy, namely, wide quantized steps lead the GH shifts to be insensitive to changing magnetic field and Fermi energy.

#### IV. CONCLUSIONS

In conclusion, we have theoretically predicted a giant quantized Goos-Hänchen (GH) effect on the surface of graphene in the quantum Hall regime. A strict model has been established and has revealed a giant quantized angular GH shift, which is dominated by a change in reflectance, for the incidence angle near the Brewster angle on reflection. The quantized steps of angular deviation have been greatly enhanced for incident angles near the Brewster angle. We have found that when the magnetic field is high or the Fermi energy is low in the quantum Hall regime, the quantized steps of Hall conductivity can be significantly widened. Meanwhile, quantized Hall conductivity is related to discrete Landau levels

in the quantum Hall regime. In addition, we have demonstrated that the cross-polarization component cannot be ignored for the incidence angle near the Brewster angle or in the case of narrow quantized steps. Also, we have found that the Brewster angle would tend to grazing incidence in the case of freestanding graphene. We can determine the quantized Hall conductivity and the discrete Landau levels by a direct optical measurement.

These findings provide a pathway for modulating the GH effect and thereby open the possibility of developing different nanophotonic devices.

#### ACKNOWLEDGMENT

This research was supported by the National Natural Science Foundation of China (Grant No. 11474089).

- 
- [1] J. D. Jackson, *Classical Electrodynamics* (Wiley, New York, 1999).
- [2] M. Born and E. Wolf, *Principles of Optics* (Cambridge University Press, Cambridge, UK, 1999).
- [3] F. Goos and H. Hänchen, *Ann. Phys. (Leipzig)* **436**, 333 (1947).
- [4] X. Yin, L. Hesselink, Z. Liu, N. Fang, and X. Zhang, *Appl. Phys. Lett.* **85**, 372 (2004).
- [5] X. Yin and L. Hesselink, *Appl. Phys. Lett.* **89**, 261108 (2006).
- [6] L. Salasnich, *Phys. Rev. A* **86**, 055801 (2012).
- [7] W. J. Wild and C. L. Giles, *Phys. Rev. A* **25**, 2099 (1982).
- [8] E. Pfleghaar, A. Marseille, and A. Weis, *Phys. Rev. Lett.* **70**, 2281 (1993).
- [9] O. Emile, T. Galstyan, A. Le Floch, and F. Bretenaker, *Phys. Rev. Lett.* **75**, 1511 (1995).
- [10] C. Bonnet, D. Chauvat, O. Emile, F. Bretenaker, A. L. Floch, and L. Dutriaux, *Opt. Lett.* **26**, 666 (2001).
- [11] P. R. Berman, *Phys. Rev. E* **66**, 067603 (2002).
- [12] D. Felbacq, A. Moreau, and R. Smaïli, *Opt. Lett.* **28**, 1633 (2003).
- [13] I. V. Shadrivov, A. A. Zharov, and Y. S. Kivshar, *Appl. Phys. Lett.* **83**, 2713 (2003).
- [14] D. Felbacq and R. Smaïli, *Phys. Rev. Lett.* **92**, 193902 (2004).
- [15] J. He, J. Yi, and S. He, *Opt. Express* **14**, 3024 (2006).
- [16] S. Longhi, G. D. Valle, and K. Staliunas, *Phys. Rev. A* **84**, 042119 (2011).
- [17] S. Grosche, A. Szameit, and M. Ornigotti, *Phys. Rev. A* **94**, 063831 (2016).
- [18] C. Xu, J. Xu, G. Song, C. Zhu, Y. Yang, and G. S. Agarwal, *Opt. Express* **24**, 21767 (2016).
- [19] C. W. J. Beenakker, R. A. Sepkhanov, A. R. Akhmerov, and J. Tworzydło, *Phys. Rev. Lett.* **102**, 146804 (2009).
- [20] S.-Y. Lee, J. Le Deunff, M. Choi, and R. Ketzmerick, *Phys. Rev. A* **89**, 022120 (2014).
- [21] H. E. Tureci and A. D. Stone, *Opt. Lett.* **27**, 7 (2002).
- [22] H. Schomerus and M. Hentschel, *Phys. Rev. Lett.* **96**, 243903 (2006).
- [23] M. Merano, A. Aiello, M. P. Van Exter, and J. P. Woerdman, *Nat. Photon.* **3**, 337 (2009).
- [24] M. Merano, N. Hermosa, A. Aiello, and J. P. Woerdman, *Opt. Lett.* **35**, 3562 (2010).
- [25] M. P. Araújo, S. De Leo, and G. G. Maia, *Phys. Rev. A* **93**, 023801 (2016).
- [26] M. P. Araújo, S. De Leo, and G. G. Maia, *Phys. Rev. A* **95**, 053836 (2017).
- [27] K. S. Novoselov, A. K. Geim, S. V. Morozov, D. Jiang, Y. Zhang, S. V. Dubonos, I. V. Grigorieva, and A. A. Firsov, *Science* **306**, 666 (2004).
- [28] A. H. C. Neto, F. Guinea, N. M. R. Peres, K. S. Novoselov, and A. K. Geim, *Rev. Mod. Phys.* **81**, 109 (2009).
- [29] F. Bonaccorso, Z. Sun, T. Hasan, and A. C. Ferrari, *Nat. Photon.* **4**, 611 (2010).
- [30] M. Merano, *Opt. Lett.* **41**, 5780 (2016).
- [31] S. Chen, C. Mi, L. Cai, M. Liu, H. Luo, and S. Wen, *Appl. Phys. Lett.* **110**, 031105 (2017).
- [32] W. J. M. Kort-Kamp, N. A. Sinitsyn, and D. A. R. Dalvit, *Phys. Rev. B* **93**, 081410 (2016).
- [33] C. C. Chan and T. Tamir, *Opt. Lett.* **10**, 378 (1985).
- [34] M. C. Chang and M. F. Yang, *Phys. Rev. B* **80**, 113304 (2009).
- [35] Y. Qin, Y. Li, H. He, and Q. Gong, *Opt. Lett.* **34**, 2551 (2009).
- [36] L. Kong, X. Wang, S. Li, Y. Li, J. Chen, B. Gu, and H. Wang, *Appl. Phys. Lett.* **100**, 071109 (2012).
- [37] X. Zhou, Z. Xiao, H. Luo, and S. Wen, *Phys. Rev. A* **85**, 043809 (2012).
- [38] X. Zhou, X. Ling, H. Luo, and S. Wen, *Appl. Phys. Lett.* **101**, 251602 (2012).
- [39] M. Pan, Y. Li, J. Ren, B. Wang, Y. Xiao, H. Yang, and Q. Gong, *Appl. Phys. Lett.* **103**, 071106 (2013).
- [40] X. Zhou, J. Zhang, X. Ling, S. Chen, H. Luo, and S. Wen, *Phys. Rev. A* **88**, 053840 (2013).
- [41] J. B. Götte, W. Löffler, and M. R. Dennis, *Phys. Rev. Lett.* **112**, 233901 (2014).
- [42] S. Grosche, M. Ornigotti, and A. Szameit, *Opt. Express* **23**, 30195 (2015).
- [43] N. Hermosa, *J. Opt.* **18**, 025612 (2016).
- [44] R. Kubo, *J. Phys. Soc. Jpn.* **12**, 570 (1957).
- [45] V. P. Gusynin and S. G. Sharapov, *Phys. Rev. Lett.* **95**, 146801 (2005).
- [46] I. Crassee, J. Levallois, A. L. Walter, M. Ostler, A. Bostwick, E. Rotenberg, T. Seyller, D. van der Mareland, and A. B. Kuzmenko, *Nat. Phys.* **7**, 48 (2011).
- [47] R. Shimano, G. Yumoto, J. Y. Yoo, R. Matsunaga, S. Tanabe, H. Hibino, T. Morimoto, and H. Aoki, *Nat. Commun.* **4**, 1841 (2013).
- [48] J. C. Martinez, M. B. A. Jalil, and S. G. Tan, *Opt. Lett.* **37**, 3237 (2012).
- [49] R. Macêdo, R. L. Stamps, and T. Dumelow, *Opt. Express* **22**, 28467 (2014).
- [50] C. F. Li, *Phys. Rev. A* **76**, 013811 (2007).
- [51] A. Aiello and J. P. Woerdman, *Opt. Lett.* **33**, 1437 (2008).

- [52] K. Y. Bliokh and A. Aiello, *J. Opt.* **15**, 014001 (2013).
- [53] H. Luo, X. Ling, X. Zhou, W. Shu, S. Wen, and D. Fan, *Phys. Rev. A* **84**, 033801 (2011).
- [54] W. K. Tse and A. H. MacDonald, *Phys. Rev. B* **84**, 205327 (2011).
- [55] W. J. M. Kort-Kamp, B. Amorim, G. Bastos, F. A. Pinheiro, F. S. S. Rosa, N. M. R. Peres, and C. Farina, *Phys. Rev. B* **92**, 205415 (2015).
- [56] L. Cai, M. Liu, S. Chen, Y. Liu, W. Shu, H. Luo, and S. Wen, *Phys. Rev. A* **95**, 013809 (2017).
- [57] M. Merano, *Phys. Rev. A* **93**, 013832 (2016).
- [58] K. Artmann, *Ann. Phys. (Leipzig)* **437**, 87 (1948).
- [59] O. J. S. Santana, S. A. Carvalho, S. De. Leo, and L. E. E. De. Araujo, *Opt. Lett.* **41**, 3884 (2016).
- [60] M. Liu, L. Cai, S. Chen, Y. Liu, H. Luo, and S. Wen, *Phys. Rev. A* **95**, 063827 (2017).